Measurement of stratospheric and mesospheric winds with a submillimeter wave limb sounder: results from JEM/SMILES and simulation study for SMILES-2

Philippe Baron[a], Naohiro Manago[b], Hiroyuki Ozeki[c], Yoshihisa Irimajiri[a], Donal Murtagh[d], Yoshinori Uzawa[a], Satoshi Ochiai[a], Masato Shiotani[e], Makoto Suzuki[f].

[a]National Institute of Information and Communications Technology (NICT), Koganei, Japan;
[b]Chiba University, Japan;
[c]Toho University, Japan;
[d] Chalmers University of Technology, Goeteborg, Sweden;
[e] Kyoto University, Kyoto, Japan;
[f]Japan Aerospace Exploration Agency, Japan;

ABSTRACT

Satellite missions for measuring winds in the troposphere and thermosphere will be launched in a near future. There is no plan to observe winds in the altitude range between 30–90 km, though middle atmospheric winds are recognized as an essential parameter in various atmospheric research areas. Sub-millimetre limb sounders have the capability to fill this altitude gap. In this paper, we summarize the wind retrievals obtained from the Japanese Superconducting Submillimeter Wave Limb Emission Sounder (SMILES) which operated from the International Space Station between September 2009 and April 2010. The results illustrate the potential of such instruments to measure winds. They also show the need of improving the wind representation in the models in the Tropics, and globally in the mesosphere. A wind measurement sensitivity study has been conducted for its successor, SMILES-2, which is being studied in Japan. If it is realized, sub-millimeter and terahertz molecular lines suitable to determine line-of-sight winds will be measured. It is shown that with the current instrument definition, line-of-sight winds can be observed from 20 km up to more than 160 km. Winds can be retrieved with a precision better than $5 \mathrm{~m \, s}^{-1}$ and a vertical resolution of 2–3 km between 35–90 km. Above 90 km, the precision is better than $10 \mathrm{~m \, s}^{-1}$ with a vertical resolution of 3–5 km. Measurements can be performed day and night with a similar sensitivity. Requirements on observation parameters such as the antenna size, the satellite altitude are discussed. An alternative setting for the spectral bands is examined. The new setting is compatible with the general scientific objectives of the mission and the instrument design. It allows to improve the wind measurement sensitivity between 35 to 90 km by a factor 2. It is also shown that retrievals can be performed with a vertical resolution of 1 km and a precision of $5–10 \mathrm{~m \, s}^{-1}$ between 50 and 90 km.

Keywords: SMILES, SMILES2, wind, stratosphere, mesosphere, thermosphere, sub-millimeter, THz, spectroscopy

1. INTRODUCTION

Middle and upper atmospheric dynamics are recognized as important issues in various atmospheric research areas such as weather and climate predictions, middle atmospheric chemistry and space weather.[1–3] Models have difficulties to simulate the dynamics in the tropics where the geostrophic wind approximation is not valid[4] and, globally, in the mesosphere and thermosphere where the winds are driven by planetary and gravity waves as well as atmospheric tides. Global observations of atmospheric winds are needed. Few satellite missions have been able to provide them, mainly in the thermosphere. Only two space missions are planned in a near future. One is the ESA Atmospheric-Dynamics-Mission (ADM) with a lidar onboard to measure winds from the surface

---

Further author information: (Send correspondence to P.B.)
P.B.: E-mail: baron@nict.go.jp

to about 20–30 km.[5] The second one is the NASA Ionospheric Connection Explorer (ICON) mission with the Michelson Interferometer for Global High-resolution Thermospheric Imaging (MIGHTI) to measure winds from 90 to 300 km (https://icon.ssl.berkeley.edu/instruments/mighti/).

The measurement gap between the troposphere and the thermosphere can be filled with a sub-millimeter (SMM) limb sounder. The technique has been successfully used to probe the middle atmospheric composition and temperature for more than 2 decades.[6–8] Horizontal winds have been derived from the Millimeter Limb Sounder (MLS) and the Submillimeter Wave Limb Emission Sounder (SMILES).[9, 10] From SMILES measurements, line-of-sight winds were retrieved from 30 km (theoretical limits of 25 km) to ≈80 km (≈100 km in night time). A ground-based millimeter radiometer has also recently been developed for wind observations in the same altitude range.[11]

Several projects have been proposed as replacement of the current SMM limb sounders but nothing has been decided yet. In Japan, SMILES-2 is being studied[12–14] and will be proposed to JAXA. The launch is planned for after 2020. The objectives are to improve the JEM/SMILES capabilities in several ways: the measurement of more species for a better characterization of the middle and upper atmosphere chemistry, the measurement of the temperature with high precision, and the extendedness of the altitude coverage up to the thermosphere. As for SMILES, SMILES-2 will use a 4-K cooled radiometer for measuring the weak signal from minor constituents. Winds are also an important target for SMILES-2 which could be the first SSM limb sounder to be designed for their measurement. In Section 2, some of the results obtained from JEM/SMILES are shown in order to illustrate the potential of such instruments to provide good quality winds. In Section 3, the current definition of the instrument and the simulation assumptions are presented. Requirements for the observation parameters are also discussed. The quantitative assessment of the wind measurement performances are described in Sect. 4 and an alternative setting for the spectral bands is proposed to improve the wind retrievals. Finally, future analyses are described in the concluding section.

2. JEM/SMILES

2.1 Measurement characteristics and retrieval method

This section presents a quick overview of the JEM/SMILES measurements processing and results. We underline the most important instrumental limitations in order to provide useful information for the preparation of SMILES-2. We use the data presented in [10]. The instrument scanned the atmospheric limb from the Earth's surface to the mesosphere. The spectra were continuously integrated and recorded every 0.5 s which corresponds to a vertical sampling of one spectrum every 2 km. The instrument field-of-view projected at the tangent point has a width of ≈4 km (FWHM). The observation parameters are given in Table 2. The emission lines of minor atmospheric constituents were observed with a spectral resolution of 1.2 MHz in three spectral bands at 625 GHz and 650 GHz. Each band has a width of 1 GHz. Figure 1 shows simulated spectra including the strongest SMILES lines, namely O_3 at 625.371 GHz and the $H^{35}Cl$ triplet at 625.92 GHz. The noise level and the spectral resolution are those of SMILES. For the tangent heights above 20 km, the atmosphere is optically thin and the signal is concentrated at the tangent point where the line-of-sight is parallel to the horizontal plane. There, the measurement is only sensitive to the horizontal components of the wind velocity. A line-of-sight wind of 5 m s^{-1} induces a frequency shift of 10^{-2} MHz.

Two line-of-sight wind profiles are retrieved from the Doppler shift of the two strongest lines, respectively. The frequency shift is inferred from the small anti-symmetrical spectral residual that remains after the retrievals of the constituents' abundance (Fig. 1). The theoretical precision (random error) is 7–9 m s^{-1} between 8 and 0.6 hPa with a vertical resolution of 5–7 km. The random retrieval errors are dominated by the measurement noise and uncertainties on the spectrometer frequencies knowledge (≈5 m s^{-1}). At higher altitudes, the random retrieval error and the vertical resolution increase up to 20 m s^{-1} and 10 km, respectively. The loss of sensitivity in the mesosphere is due to the weakness of the measured lines and to the spectral resolution (1.2 MHz) that is similar to the lines width. In night time, retrievals can been performed up to 90-100 km (10^{-3} hPa) using the signal increase due to the secondary O_3 peak. Below 30 km, the spectral signature of the Doppler-shift is flatten because of the broadening of the spectral line (≈ 20 MHz) and becomes difficult to fit. Note that the

low retrieval performances below 30 km is has been found throughout the whole millimeter and sub-millimeter spectrum for retrievals with spectral bandwidth smaller 10 GHz.[15] The only way to improve the performances is to use very large spectral bandwidth (>20 GHz) in order to increase the number of molecular lines with moderate intensities.

A large bias of 20–40 m s^{-1} is found on the retrievals. It is mitigated considering that the daily average of the tropical meridional winds is near zero. The SMILES winds are adjusted with respect to daily averaged ECMWF analyses of tropical meridional winds. Several sources of the bias have been identified. At 50 km (Fig. 5 in[10]), the average differences between retrievals from the O_3 line simultaneously measured with the two Acousto-Optical Spectrometers (AOS) are 20–30 m s^{-1} suggesting that the AOS's are the dominant source. The simultaneous measurements of the O_3 line was performed when the so-called bands A and B are measured. Bands A and B are the symmetric bands about a secondary local oscillator. Retrievals from the two bands show some opposite variations (<10 m s^{-1}) over time scales of <2 weeks likely due to variations of the secondary local oscillator frequency. A slow frequency drift of 20 m s^{-1}/6 months was detected for the two bands which is attributed to the expected drift of the main local oscillator frequency (use to separate bands A/B and C). Note that a new version of the level-1b data is now available with significant improvements of the intensity calibration and AOS frequency calibration. These results suggest that the total retrieval bias is dominated by the AOS spectrometer frequencies errors. The bias correction also removes errors from the satellite velocity along the line-of-sight (4 km/s) and error on the spectral line frequency. As shown in the results presented in the next session, the zero-wind correction is efficient below 50–60 km (errors less than 2 m s^{-1}) but can have larger uncertainties in the mesosphere ($\approx$5–10 m s^{-1}) which are difficult to identified because of a lack of good references.

2.2 SMILES "zonal" and "meridional" winds

The zonal wind is not measured with JEM/SMILES but in the descending branch of the orbit, the line-of-sight direction is oriented near the zonal direction within $\pm 10°$ (Fig. 2). Figure 3 shows daily and zonally averages of SMILES line-of-sight winds measured near the zonal direction at 6.6 hPa (≈ 35 km) and 1 hPa (≈ 50 km). The semi annual oscillation of the zonal wind is seen in the tropics near the stratopause while, at the highest latitudes observed with SMILES (55°N), the reversal of the zonal wind after the major sudden stratospheric warming on 24th of January (vertical balck line) is measured. Two minor warmings are also seen in November and December, respectively.

SMILES data are compared with the line-of-winds computed from the operational wind analyses by the European Centre for Medium-Range Weather Forecasts (ECMWF). SMILES single profiles and collocated ECMWF ones are paired and average in the same way.[10] In mid-latitudes and at 1 hPa, the differences between the two line-of-sight winds are on average 2 m s^{-1} (horizontal dashed-lines). This good agreement suggests the good quality of both SMILES measurement and ECMWF forecast in this region. At 7 hPa, ECMWF analyses do not reproduce the reversal of the wind direction after the stratospheric warming. Above the Equator, the differences between SMILES and ECMWF can be more than 10 m s^{-1}. The differences are likely due to the difficulties of ECMWF to correctly reproduce the winds in the Tropics where the geostrophic wind approximation is not valid.

In the mesosphere (Fig 4), SMILES and ECMWF zonal winds exhibit large differences (> 20 m s^{-1}), especially in the tropics. In particular SMILES observations show larger variabilities on small time scales of 1–2 week. They are likely due to the parametrization of the atmospheric tides and planetary waves in the ECMWF analyses.

Figure 5 shows the zonal-average of line-of-sight winds when the line-of-sight is oriented near the meridional direction (ascending orbit branch in Fig. 2). The line-of-sight winds are shown in the tropics and the extra-tropics. They have been retrieved from the HCl lines and zonally averaged per periods of 5 days. The observations are shown at different times regularly distributed over 2 months, which corresponds to a complete diurnal cycle of the local time. Clear vertical oscillations are visible on the plots. They are anti-symmetric with respect to the Equator and their amplitudes increase with the altitude up to velocities larger than 20 m s^{-1} at 80 km. The vertical period is 10–20 km. The first and last panels show the observations at almost the same local times and, though they are separated by a period of 2 months, the wind patterns are similar. This indicates a cyclic variation of the vertical oscillations with a period of 24-hours (local time). These characteristics are typical of the effects expected from migrating tides.
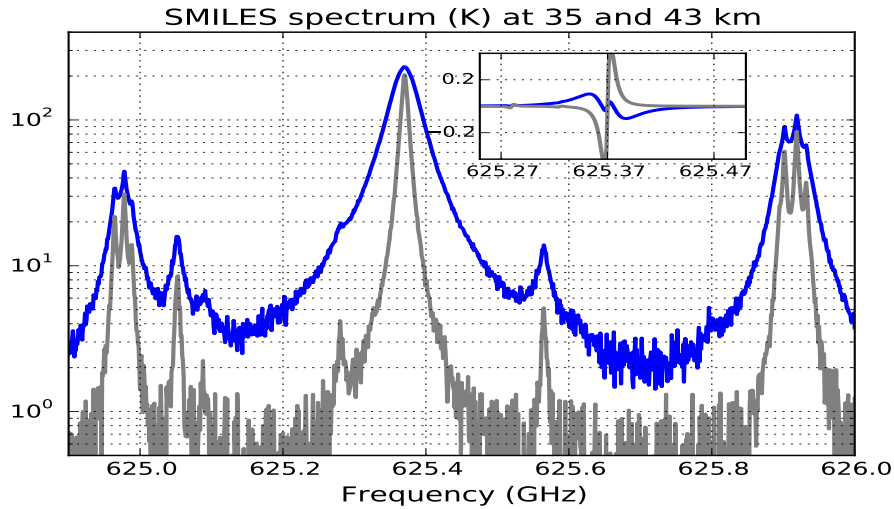
Figure 1. Simulated SMILES spectra at tangent heights of 35 and 44 km (blue and grey lines, respectively). The intensity is expressed in brightness temperature (K). The encrusted panel shows the differences between the spectra calculations with and without wind. The wind profile is set to 10 m s^{-1} below 40 km and -10m s^{-1} above
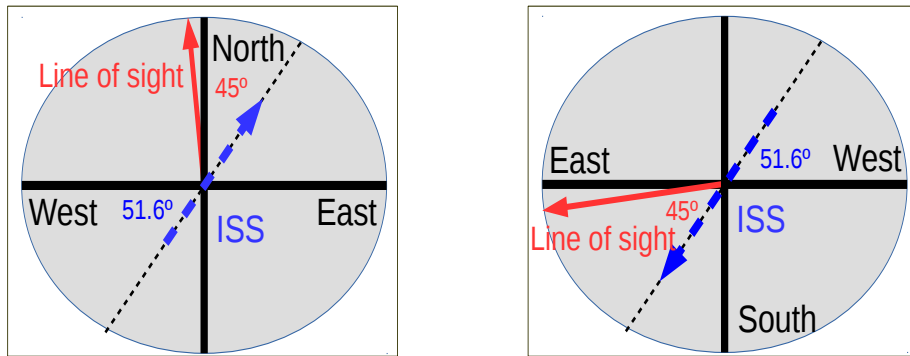

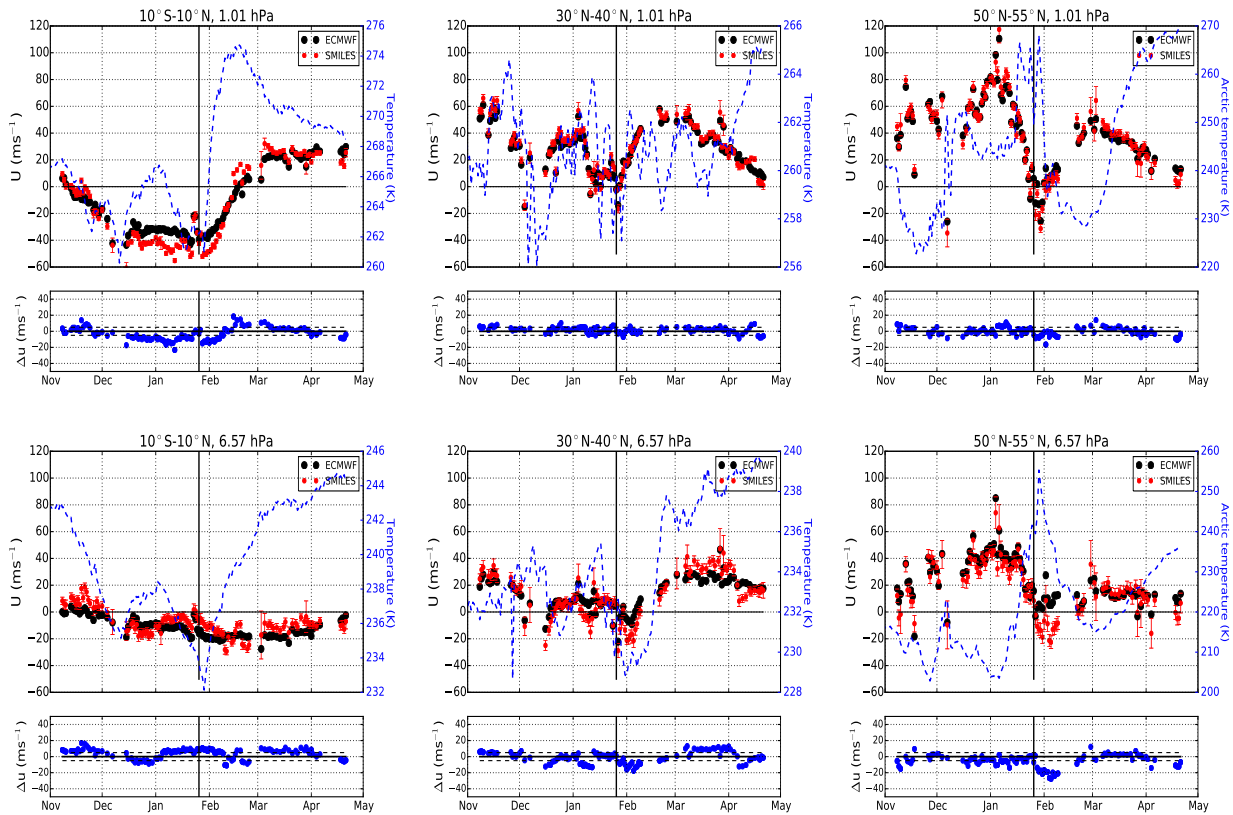Figure 2. Line-of-sight orientation when the ISS is on the ascending (left panel) and descending (right panel) orbit branch.

Figure 3. Zonally and daily average of the line-of-sight winds measured by JEM/SMILES with a line-of-sight orientation between $\pm 10°$ from the zonal direction. Observations in the equatorial, mid-latitudes and subarctic regions are shown from left to right. The upper and lower panels show the results at the altitudes of 6.6 hPa (≈ 35 km) and 1 hPa (≈ 50 km), respectively. The red dots are the SMILES measurements and the black dots are the average of the collocated line-of-sight winds derived from the ECMWF operational analyses. The blue dashed lines are the temperature zonal-means derived from the AURA/MLS measurements (version 3.3). The mean temperatures are calculated in the same latitude ranges as the SMILES data except for the subarctic region panels which show the mean temperatures at latitudes $>60°$N. The vertical black line indicates the major sudden stratospheric warming event on 24th of January. The differences between SMILES and ECMWF winds are shown in the smallest panels. The horizontal dashed lines show the range ± 2 m s^{-1}.
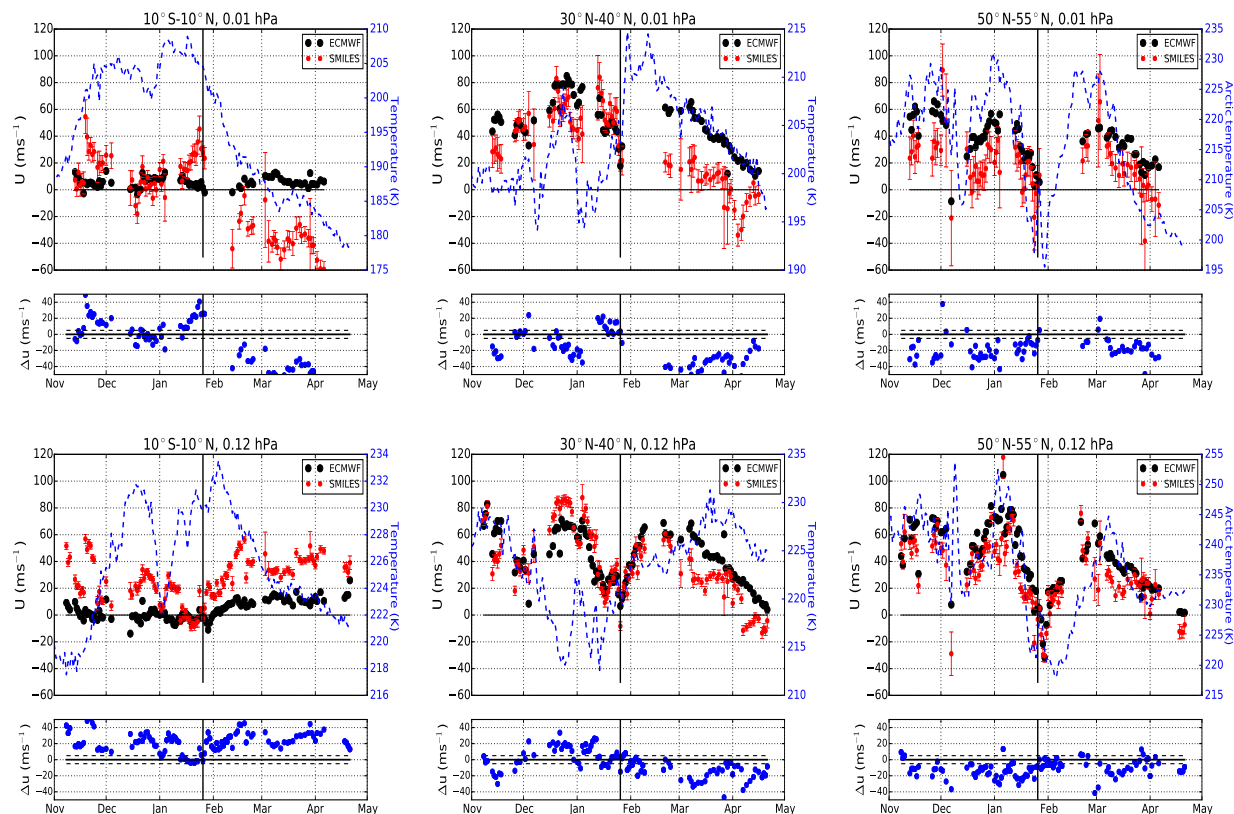
Figure 4.   Same as for Fig. 3 but for altitudes at 0.1 hPa (≈60 km, two lowermost panels) and 0.01 hPa (≈75 km, two uppermost panels).

3. SMILES-2

3.1 Instrument characteristics

The current definition of SMILES-2 includes 6 spectral bands near 500 GHz, 630 GHz and 2 THz (Table 1). The bands have been selected for measuring temperature, a large number of important reactive species as well as, for the first time on a global scale, the atomic oxygen in its fundamental state.[12–14] Line-of-sight wind is also one of the important targets of SMILES-2. Figure 6 shows synthetic spectra of the bands with the main molecular lines. Weak spectral lines including those of scientifically important species such as BrO are not included. As for JEM/SMILES, the radiometer will be cooled at 4 K in order to obtain the high precision required to measure the low signal associated with most of the targets (e.g., BrO, NO_2, wind, mesospheric ozone). Two Superconductor-Insulator-Superconductor (SIS) mixers are used to measure 4 spectral sub-mm bands and one Hot Electron Bolometer for two THz bands. In this study, we consider two pairs of bands made of bands 1 and 2 (487 and 525 GHz) and 3 and 4 (625 and 650 GHz), respectively. The paired bands are measured together with a double-sideband radiometer. The two THz bands are measured one at the time with a single-sideband radiometer. It is planned to use three digital spectrometers (fast-Fourier-transform or autocorrelator types). We consider that the sub-millimeter bands are measured with a bandwidth of 4 GHz and a resolution of 0.25 MHz, i.e., 8000 frequencies per spectrum. A bandwidth of 2 GHz and a resolution of 0.5 MHz are considered for the THz bands. The spectral resolution is enough since the width of THz lines are larger than 1 MHz (Eq. 1). For example, the half-width-half-maximum (HWHM) of the Doppler-broadened atomic oxygen line is w_{dop}=2.5 MHz at 2 THz and at a temperature of 200 K. That of an O_3 line is w_{dop}=1.3 MHz at 2 THz (same temperature) and w_{dop}=0.4 MHz at 600 GHz.
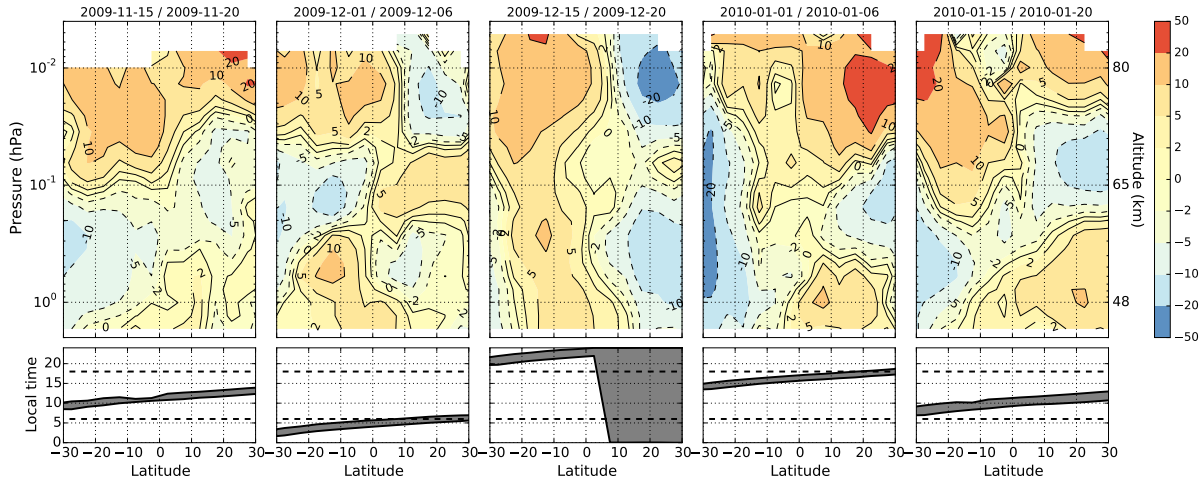
Figure 5. Zonal mean of the line-of-sigh winds ($\mathrm{m\,s^{-1}}$) between $30°\mathrm{S}$–$30°\mathrm{N}$ and from 2009-11-15 to 2011-01-20 measured with JEM/SMILES pointing near the meridional direction. Data are retrieved from the $H^{35}Cl$ line. The time range correspond to 24-hour variation of the local time. Each panel corresponds to the average of 5 days observations. The lower panels indicate the local time of the measurements.

$$w_{dop} \;=\; \frac{\nu}{c}\,\sqrt{\frac{2\ln 2\,R\,T}{M}}, \tag{1}$$

with ν the frequency (Hz), $c = 2.99792458 \times 10^8$ $\mathrm{m\,s^{-1}}$ is the light velocity in the vaccum, R=8.3145 $\mathrm{J\,K^{-1}\,mol^{-1}}$ is the gas constant, T is the temperature (K) and M ($\mathrm{kg\,mol^{-1}}$) is the molar mass.

The most promising lines for wind measurements are the O_2 and H_2O lines at 488 GHz, the O_3 and HCl lines in bands 3 and 4, and the atomic oxygen line at 2.06 THz (Fig. 6). Notice that the 488 GHz lines have already been measured with Odin/SMR[16,17] while the lines between 624–626 GHz have been measured with JEM/SMILES.[8] Compared to JEM/SMILES, significant improvements of the wind measurement performances are expected. Here below we point out the most interesting aspects of SMILES-2 compared to JEM/SMILES:

- The use of a digital spectrometers will mitigate a large part of the JEM/SMILES retrieval errors induced by the optical spectrometers.

- The larger number of lines with intensity similar to the JEM/SMILES O_3 and HCl lines will improve the retrieval performances in the stratosphere.

- The strong O_2 line will give a much stronger signal in the middle and upper mesosphere.

- The better spectral resolution will improve the retrievals in the mesosphere.

- The atomic oxygen line will provide, among others, wind information in the thermosphere.

3.2 Simulation characteristics

Here the measurement performances are defined by the precision and the resolution of the retrieved line-of-sight wind profile. They depend on the instrument noise, the instrument vertical resolution and the atmospheric
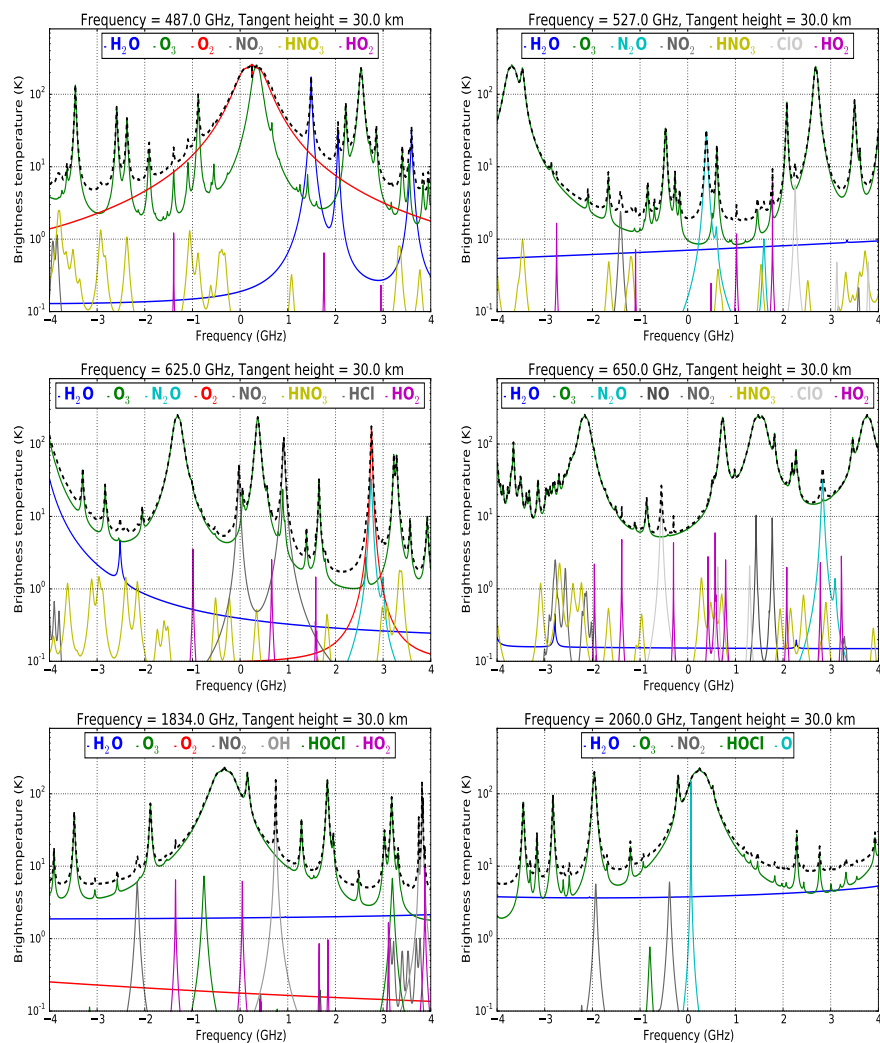
Figure 6. Synthetic spectra of the bands selected for SMILES-2 at a tangent height of 30 km. The full-lines show the lines of the main species and the dashed-black lines show the total intensity. Weak lines such as BrO and H_2CO at 525 GHz, and HOCl at 625 GHz are not included.
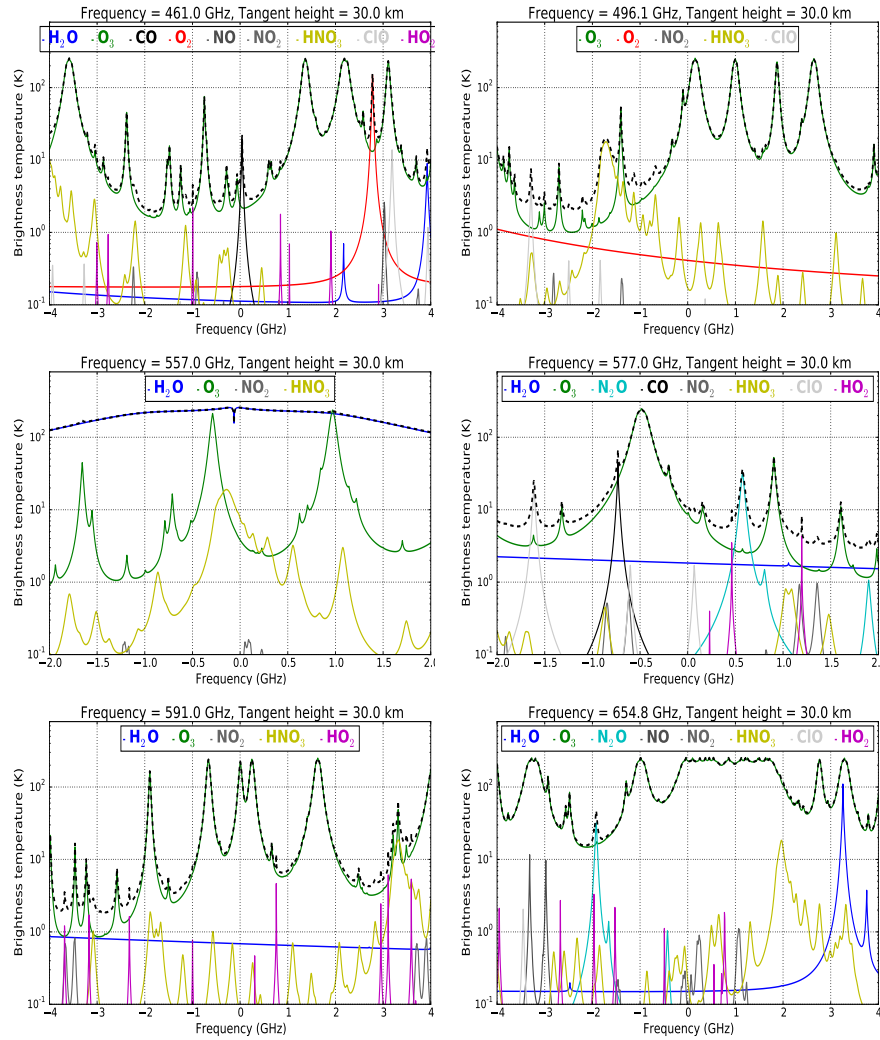
Figure 7. Same as Fig. 6 but for alternative wind observation bands.

Table 1. Radiometer characteristics for SMILES-2[1]

SIS-1, DSB, $Tsys^{dsb}$=150 K	
4 GHz bandwidth, 0.25 MHz resolution	
(1) 485-489 GHz	T, Wind, O_2, H_2O, O_3, HO_2
(2) 525-529 GHz	BrO, NO_2, H_2CO, N_2O, HO_2
SIS-2, DSB, $Tsys^{dsb}$=150 K	
4 GHz bandwidth, 0.25 MHz resolution	
(3) 623-627 GHz	O_3, HCl, BrO, HNO3, HO_2, N_2O, HOCl, CH_3Cl
(4) 648-652 GHz	O_3, ClO, HO_2, BrO, NO
HEB, SSB, $Tsys^{dsb}$=1000 K	
1 GHz bandwidth, 0.5 MHz resolution	
(5) 2.06 THz	O-atom, upper atmospheric wind and temperature
(6) 1.8 THz	OH, H_2O, O_3

[1]The spectral resolution if 0.5 MHz for all bands.

Table 2. Observation characteristics[1]

Antenna diameter (vertical axis)	1 m (40 cm)
Antenna FOV FWHM	0.035° at 600 GHz (0.09°)
Platform altitude	400 km (350 km)
Vertical velocity	$0.1°\,s^{-1}$ ($0.11°\,s^{-1}$)
Spectrum integration time	0.1 s (0.5 s)
Vertical sampling	0.38 km
Limb resolution at 30 km	1.34 km at 600 GHz (4.1 km)
	0.4 km at 2 THz
Atmospheric scan duration	≈30 s for 120 km vertical range
Calibration phase duration	25 s for JEM/SMILES
along-track sampling	≈450 km for JEM/SMILES
Scans per day	≈1600 for JEM/SMILES

[1]The parameters for JEM/SMILES are given in parenthesis

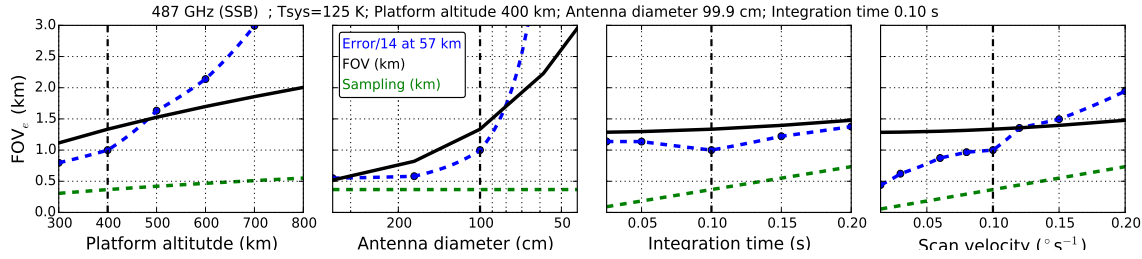Figure 8. From left to right: instrument vertical FWHM (blacl lines), vertical sampling (green dashed lines) and wind retrieval errors at 57 km (cirles blue lines) with respect to the satellite altitude, antenna diameter, spectrum integration time and vertical scan velocity. The errors are estimated for a SSB measurement of band-1 (487 GHz) with parameters in Tab 1–2. The vertical dashed-lines show the default values of the observation parameters.

conditions. The measurement noise associated with a double sideband (DSB) spectrum is estimated from the radiometer system temperature T_{sys}^{dsb} as:

$$\sigma_m^{dsb} = \frac{T_{sys}^{dsb} + T_{atm}^{dsb}}{\sqrt{w \times \Delta_T}}, \tag{2}$$

where σ_m^{dsb} is the DSB noise standard deviation, w is spectral resolution (Hz), Δ_T is the spectrum integration time and T_{atm}^{dsb} is the DSB atmospheric signal intensity. The atmospheric radiance is expressed in the so called "brightness temperature" used in most of the literature. It is a linear conversion of the radiance unit to a temperature unit using the Rayleigh-Jean transformation. The two image bands composing a DSB spectrum have the same weight such that:

$$T_{atm}^{dsb}(F_i) = \frac{1}{2} \left(T_{atm}(F_{lo} - F_i) + T_{atm}(F_{lo} + F_i) \right), \tag{3}$$

where $T_{atm}(F)$ is the signal intensity at the frequency F captured by the antenna, F_i and F_{lo} are the intermediate and local oscillator frequencies. The intermediate frequency is in the microwave domain. For a single-sideband (SSB) mode, the error standard deviation σ_m^{ssb} is:

$$\sigma_m^{ssb} = \frac{2\,T_{sys}^{dsb} + T_{atm}}{\sqrt{w \times \Delta_T}}. \tag{4}$$

For the sub-mm bands, we consider a value of T_{sys}^{dsb} of 125 K and, for the THz ones a value of 1000 K. Those values are based on the performances obtained with past instruments. In the sub-mm domain, JEM/SMILES and Herschel/HIFI[18] system temperatures were about 150 K and 100 K, respectively. In the THz domain, Herschel/HIFI had a DSB system temperature <1000 K at 2 THz. and NICT has developed a HEB receiver at 3 THz with a DSB system temperature of 1200 K. Those values correspond to the radiometer noise level and they should be increased by about ≈20% in order to take into account an additional noise due to the calibration procedure. We should also bear in mind that instrument performances improve regularly with time, especially in the THz domain.

The vertical resolution of the instrument is characterized by the full-width-half-maximum (FWHM) of the effective field-of-view, FOV_e (deg). It depends on the static antenna FOV and the line-of-sight vertical motion. It can can be approximated as:

$$\text{FOV}_e = \sqrt{\text{FOV}^2 + \left(\dot{\theta}\,\Delta_T \right)^2} = \sqrt{4891 \left(\tfrac{\lambda}{D} \right)^2 + \left(\dot{\theta}\,\Delta_T \right)^2}, \tag{5}$$

where λ (m) is the wavelength, D (m) is the antenna diameter, $\dot{\theta}$ (°/s) is the vertical scan velocity. The instrument vertical resolution Δ_L (km) at the limb can be approximated from simple geometry calculations by:

$$\Delta_L \approx 1.9\sqrt{Z_{sat}}\,\mathrm{FOV}_e, \tag{6}$$

where Z_{sat} (km) is the satellite altitude above the surface. The observation parameters assumed in this study are given in Table 2. We consider an antenna diameter of 1 m which is larger than that of JEM/SMILES (40 cm) but similar to the Odin one. The integration time is 0.1 s, much smaller than that of JEM/SMILES (0.5 s). The scan velocity and the satellite altitude are similar to JEM/SMILES. The instrument limb resolution is $\approx$1.34 km and the tangent height sampling of $\approx$0.38 km. Figure 8 shows how the instrument vertical resolution for band 1 (487 GHz) varies with the observation characteristics. The change of the retrieval error is also shown. The error calculation will be described in the next section. It should be noticed that the wind profile can be retrieved with a higher vertical resolution than that of the instrument. The vertical information is given by the tangent-height vertical sampling ($\dot{\theta}\,\Delta_T$) and the spectral line shape where the line broadening is dominated by pressure. However the cost in term of precision is high. For wind retrieved with sufficient signal, the best compromise between the retrieval vertical resolution and the retrieval error is obtained if the retrieval vertical resolution matches that of the instrument. For example, increasing the antenna diameter from 1 m to 1.6 m increases the instrument vertical resolution from 1.4 to 1 km and, the retrieval error for vertical resolution of 1 km decreases by almost a factor 2 (second panel of Fig. 8).

A climatology of the most important species and atmospheric parameters related to wind retrievals have been created to represent winter, day and night conditions, and 11 latitudes between 80°S and 80°N. The altitude range is 10–400 km (Fig. 9). We have chosen one of the solstice seasons because of the high contrast between the winter-pole and summer-pole conditions which provides a large range of atmospheric states. Day and night states are separated because of the large diurnal variation of O_3 in the mesosphere. The climatology fairly described the atmospheric conditions for the sensitivity study presented in this paper. It will be improved in the future, especially in the altitude range between 80 and 150 km. Constituents such as NO+ will also be included in the future for extending the study to other potential products. Data for O_3, H_2O, CO, HCl, temperature and pressure have been derived from the AURA/MLS observations (version 3.3, November-15 2009 to February-15 2010) at altitudes below 90 km. Data with large a priori contaminations are kept to prevent any gap in the profiles. Temperature pressure, atomic and molecular oxygen are taken from the Ground-to-topside model of Atmosphere and Ionosphere for Aeronomy (GAIA).[3] Though CO is produced in the thermosphere, neither MLS nor GAIA provide thermospheric concentration. Here, we simply extrapolate the MLS profiles up to 150 km in order to represent the high thermospheric CO abundance according to values found in the literature. For other species, the abundances are exponentially decreased in the altitude range where no information is available.

4. WIND MEASUREMENT PERFORMANCES

4.1 Retrieval performances calculation

The retrieval errors are assessed using the optimal estimation method.[19] The total retrieval error covariance matrix $\mathbf{Sr}$ is given by the equation:

$$\mathbf{Sr} = \mathbf{D\,Sy\,D}^T + (1 - \mathbf{D\,K})\,\mathbf{Sx}\,(1 - \mathbf{D\,K})^T, \tag{7}$$

where $\mathbf{Sx}$ and $\mathbf{Sy}$ are the covariance matrices associated with the a priori wind profile and the measurement error, respectively. Both matrices are diagonal and $Sy[i,i] = \left(\sigma_m^{ssb,dsb}\right)^2$. The matrix $\mathbf{K}$ is the Jacobian matrix of the measurement and $\mathbf{D} = (\mathbf{K}^T\mathbf{Sy}^{-1}\mathbf{K} + \mathbf{Sx}^{-1})^{-1}\mathbf{K}^T\mathbf{Sy}^{-1}$. These matrices as well as the simulated spectra are computed using the Advanced Model for Atmospheric Terahertz Radiation Analysis and Simulation (AM-ATERASU)[20, 21] used in the SMILES research processing chain.[22] The spectroscopic line parameters are taken from the version 2008 of the HITRAN catalog.[23]

Following the retrieval strategy used for JEM/SMILES, we consider that a wind profile is retrieved alone. Only the measurement noise is taken into account since it is the most important error source in the JEM/SMILES
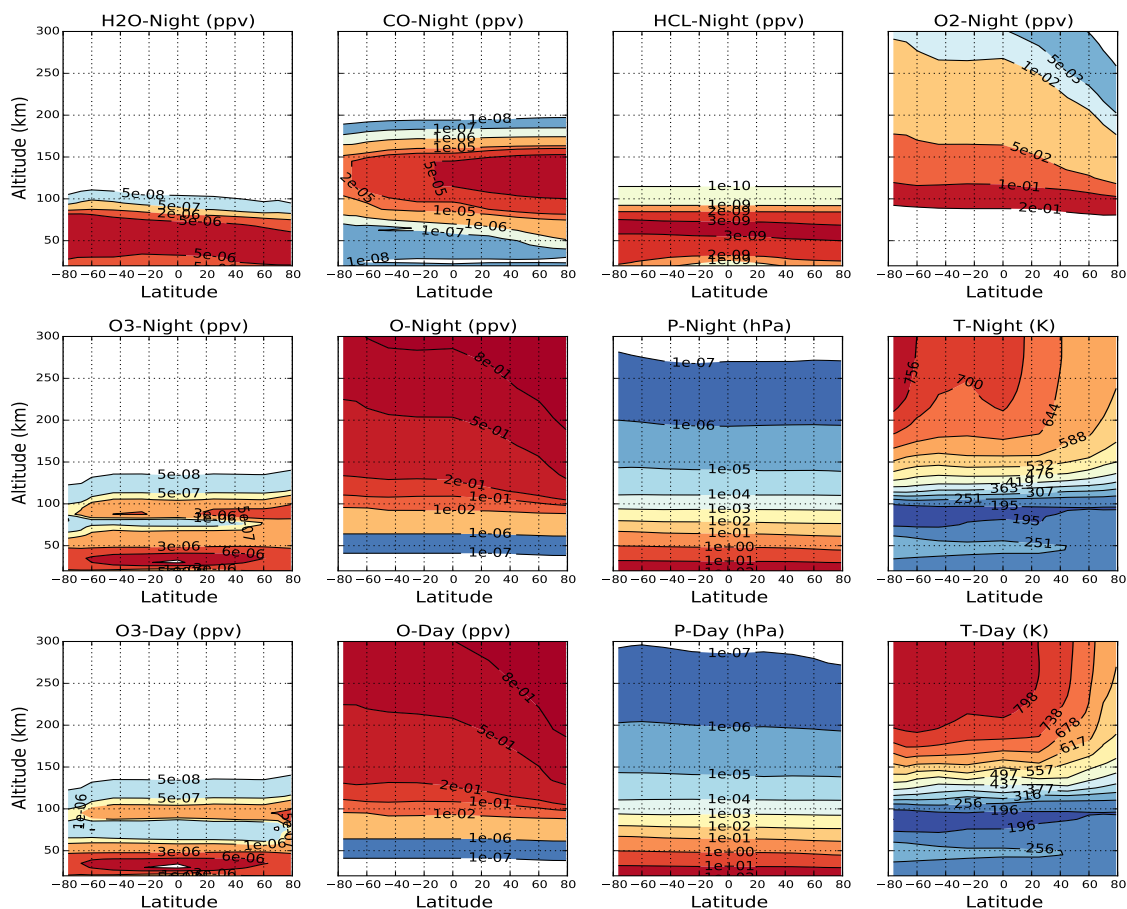
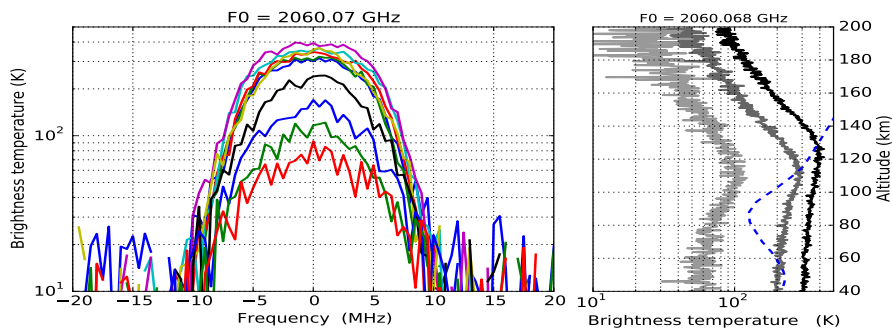Figure 9. Atmospheric profiles used for the simulations.

Figure 10. Simulation of the atomic oxygen line measurements. The right panel shows the spectra for tangent heights ranging from from 40 km to 200 km. The left panel shows the vertical profiles of radiances at the line center (black line), at 5 MHz from the line center (grey line) and 7.5 MHz from the line center (light grey).
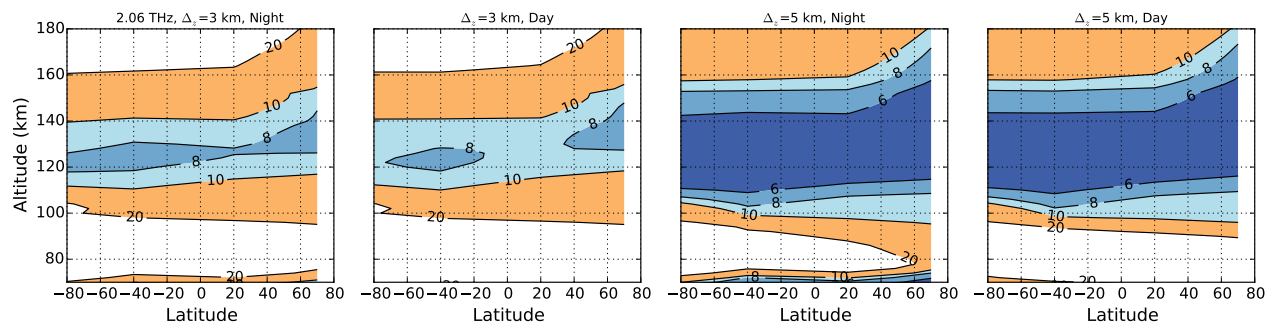
Figure 11. Latitude and altitude distribution of the line-of-sight wind measurement errors $(\mathrm{m\,s^{-1}})$ estimated for band-5 (2.06 THz, SSB) and for retrievals with a vertical resolution of 3 km (two left-most panels) and 5 km (two right-most panels). Calculations are performed for night and day times.
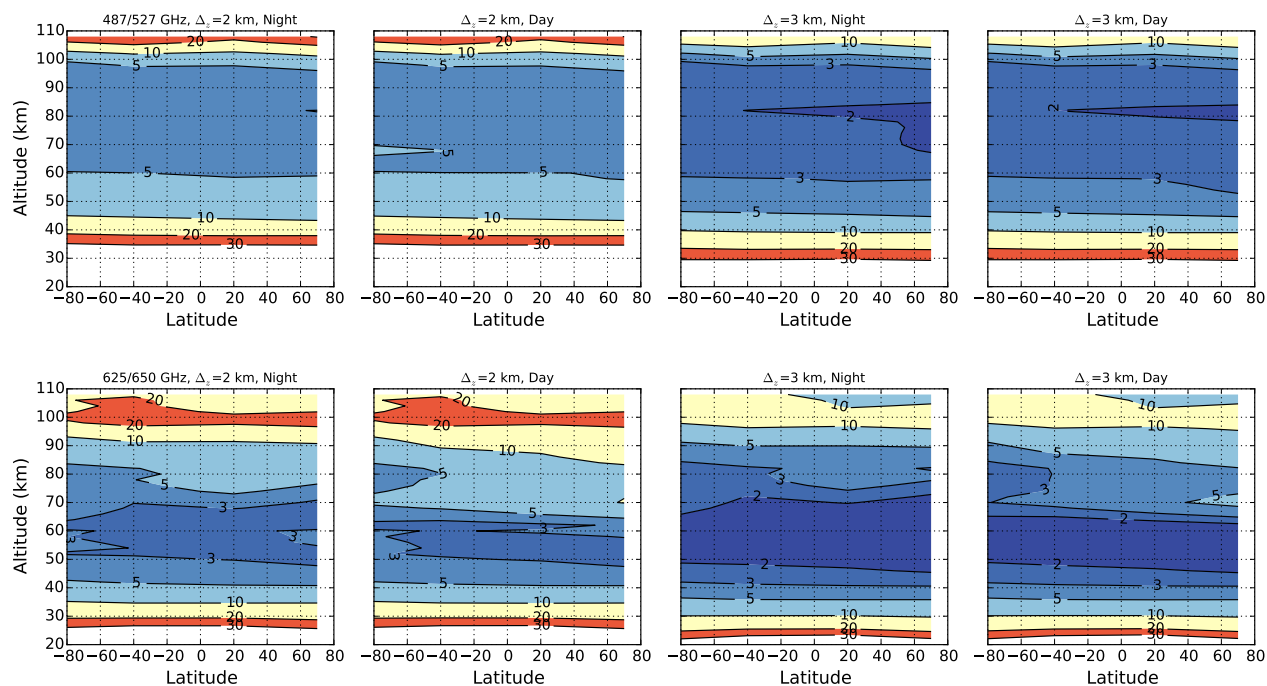

Figure 12. Latitude and altitude distribution of retrieval errors $(\mathrm{m\,s^{-1}})$ estimated for bands 1–2 (487/527 GHz, DSB) (upper panels) and bands 3–4 (625/650 GHz, DSB) (lower panels). Results are shown for day and night times and for retrieval vertical resolutions of 2 km (two left-most panels) and 3 km (two right-most panels).

retrievals (together with the errors originated from the optical spectrometers but which can be ignored for SMILES-2). The noise is responsible of a random error and it characterizes the precision of the retrievals. Other errors such as the ones on the intensity calibration, spectroscopic parameters and line-of-sight velocity correction are responsible for a retrieval bias and to some extend, can be reduced to an acceptable level ($<2\,\mathrm{m\,s^{-1}}$) with the definition of the instrument. The retrieval biases will be analysed in future works. A very large and unrepresentative a-priori error ($\mathbf{Sx}$) of $1000\,\mathrm{m\,s^{-1}}$ is used but only retrievals with a total retrieval error ($\mathbf{Sr}$) less than $20\,\mathrm{m\,s^{-1}}$ are considered as good retrievals. The impact of the a priori regularization on the good retrievals is negligible and the vertical resolution of the retrieved profile is that of the retrieval altitude grid. The retrieval precision is given by the square-root of the diagonal elements of $\mathbf{D\,Sy\,D}^T$ (measurement induced error in Eq 7).

4.2 Results for the default spectral bands

Figure 11 shows the line-of-sight wind retrieval errors from band-5 (2.06 THz). The information is mainly taken from the atomic oxygen line (Fig. 10). The retrieval precision from about 100 to 160 km is between 4–$10\,\mathrm{m\,s^{-1}}$ with a vertical resolution between 3–5 km. Below 100 km, the signal intensity becomes insufficient for wind retrievals because the atmosphere is opaque near the line center and the concentration of atomic oxygen strongly decreases. The altitude range of good retrievals is wider at the winter-pole (upper boundary at $\approx$180 km), a region characterized by a descent of air rich in atomic oxygen (Fig:9). No strong differences can be noticed between the day and night conditions. The theoretical retrieval performances are close to those expected for the Michelson Interferometer for Global High-resolution Thermospheric Imaging (MIGTHTI) onboard the satellite ICON (https://icon.ssl.berkeley.edu/instruments/mighti/). MIGHTI will measure the wind vector components between 90–300 km but only in night time between 105–200 km. Between 90 and 160 km, the precision is estimated to 4–$6\,\mathrm{m\,s^{-1}}$ with a vertical resolution of 2.5 km and a horizontal resolution of 500 km.

Figure 12 shows the line-of-sight wind retrieval errors from the sub-millimetre spectra (bands 1–2 and 3–4). Errors better than $5\,\mathrm{m\,s^{-1}}$ are obtained between 40 and 100 km with a vertical resolution of 2–3 km. Above 70 km, the information is provided by the O_2 line in band-1 and for altitudes below, the information is taken from the O_3 lines in bands 1,3 and 4 and to a less extend from the band-1 O_2 and water vapour lines. Band-3 (527 GHz) does not help for retrieving winds. Between 60 and 70 km, a significant loss of sensitivity is seen for the retrieval from bands 3-4 which is due to the large decrease of the O_3 abundance in day time. The altitude range with the best wind retrievals is found between 50–70 km with a precision better than $3\,\mathrm{m\,s^{-1}}$ and a vertical resolution of 2 km. It is a region where current wind observation techniques lack sensitivity.[15]

4.3 Results for the alternative bands

We performed a spectral survey to identify the best bands to be paired with the SSM bands selected for SMILES-2. The search range is limited to $\pm$40 MHz from the SMILES-2 band center. Figure 13 shows the errors for bands 1, 3 and 4. Errors are estimated at altitudes of 30 and 54 km for a retrieval vertical resolution of 3 km. The errors from the SSB retrievals are used as reference (dashed lines).

At 30 km, the information is provided by lines with moderate intensity, mostly O_3 lines. These lines are regularly distributed in the entire sub-millimetre spectrum and, consequently, most of the bands can be associated with a SMILES-2 band to improve the wind retrievals. A 8-GHz SSB retrieval (the two right-most panels) provides similar results as a 4-GHz DSB (the two left-most panels). The 527 GHz band is one of the rare bands that does not improve the wind retrievals. However we should bear in mind that, because of the absence of strong lines, this band is interesting for sounding the upper troposphere and lower stratosphere composition, in particular the dynamical tracer N_2O as well as species with very weak lines (e.g., BrO, H_2CO). The pair 625/650 GHz with 4 GHz bandwidth gives an error of $9\,\mathrm{m\,s^{-1}}$, close to the best candidate paired bands 591/625 GHz (7–$8\,\mathrm{m\,s^{-1}}$). The poor performances at 30 km have also been reported from a survey through the whole millimetre and THz spectrum.[15] Considering that increasing the bandwidth by a factor 2 allows to reduce the retrieval error by a factor $\sqrt{2}$, it is necessary to use DSB spectra with a bandwidth larger than 16 GHz to reach an error smaller than $5\,\mathrm{m\,s^{-1}}$ at 30 km.

At 50 km, retrieval performances depend on the presence of strong lines which are irregularly distributed. Only few bands can improve the retrievals and increasing the bandwidth does not necessarily help. The most interesting spectral range is the dense cluster of O_3 lines at 655 GHz (Fig. 7). For frequencies lower than 700 GHz,
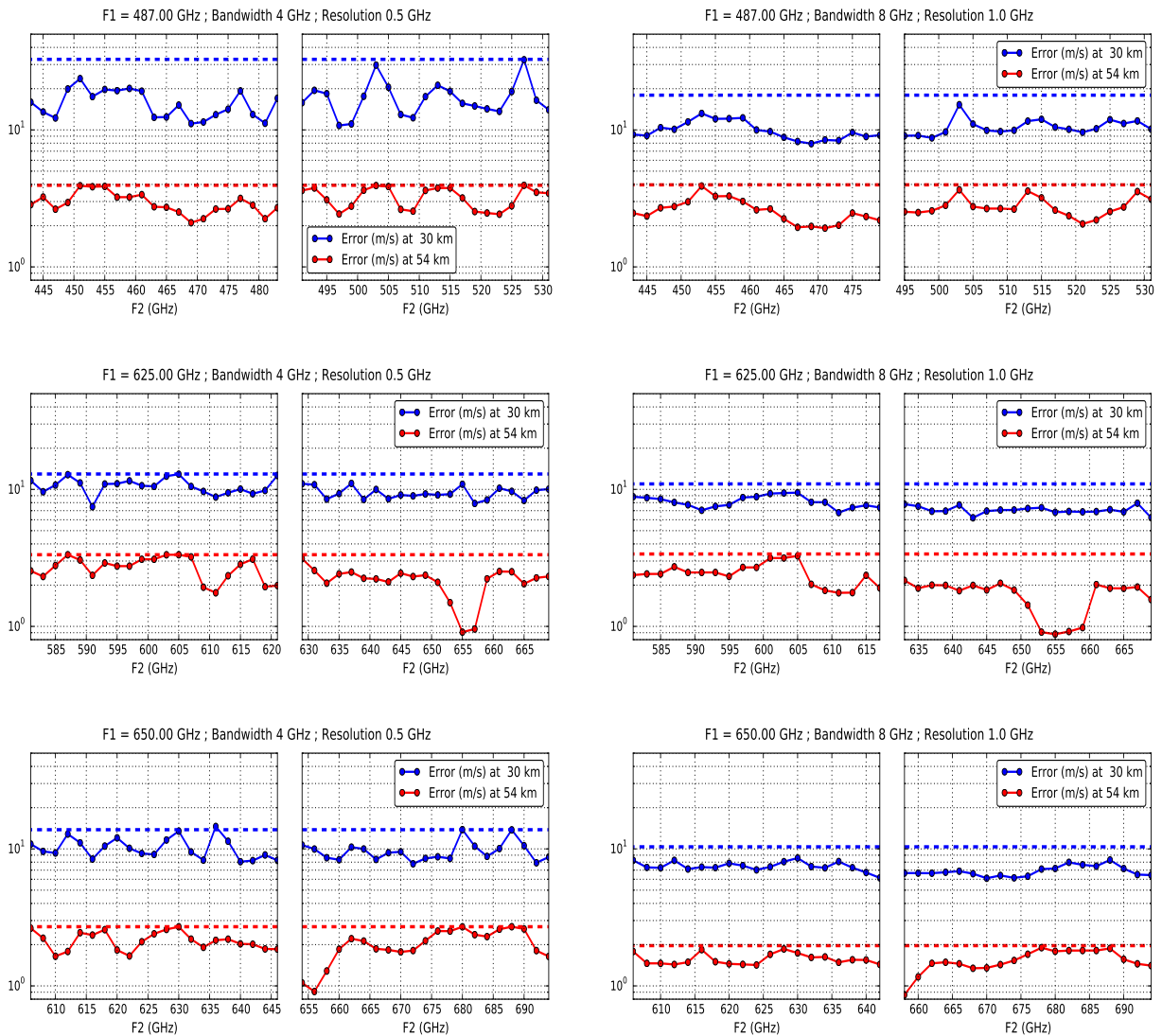
Figure 13. First row: Wind retrieval errors at 30 and 54 km with 3 km retrieval vertical resolution for a double-side band measurement of band-1 (487 GHz) with respect to the image band central frequencies (F_2). The dashed lines show the errors for a single-side band measurement. The two left-most panels are the errors for 4 GHz bandwidth and the two right-most ones are errors for 8 GHz bandwidth. Second and third rows: same as first row but for band-3 (625 GHz) and band-4 (650 GHz), respectively.
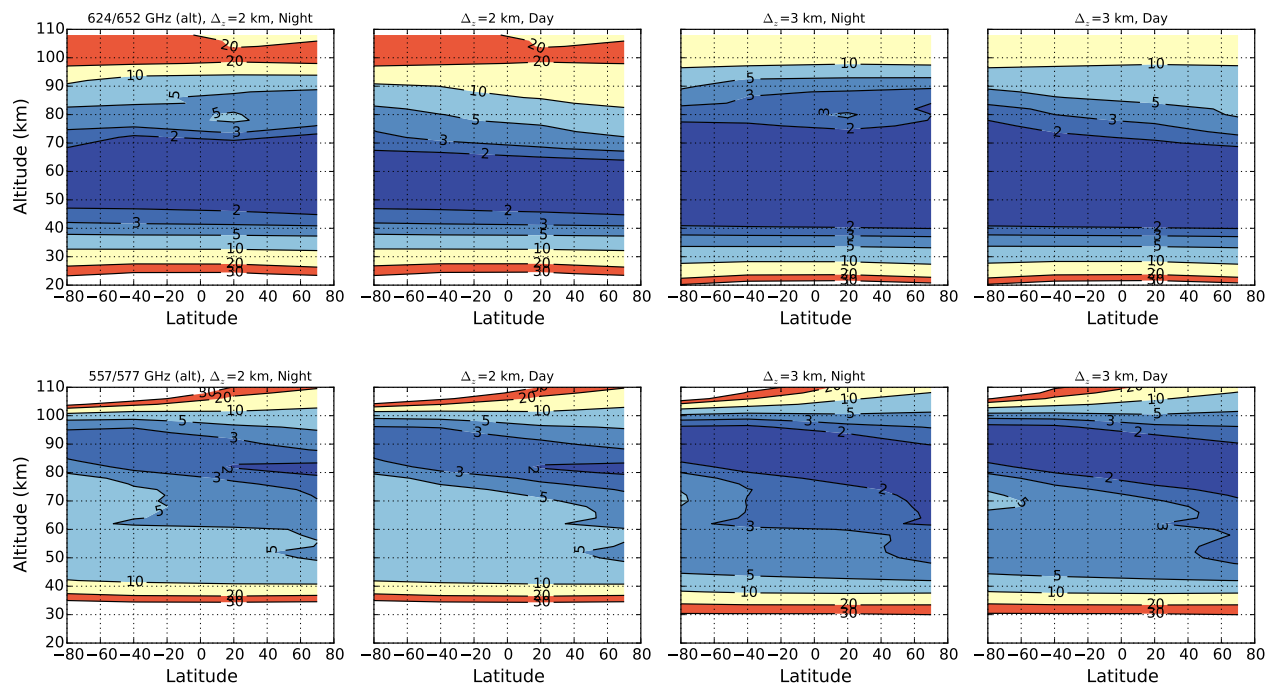
Figure 14. Same as Fig. 12 but for the alternatives bands: 624/652 GHz, DSB, 8 GHz bandwidth, 1 MHz resolution (upper panels), and 557/577 GHz, DSB, 2 GHz bandwidth, 0.25 MHz resolution (lower panels).
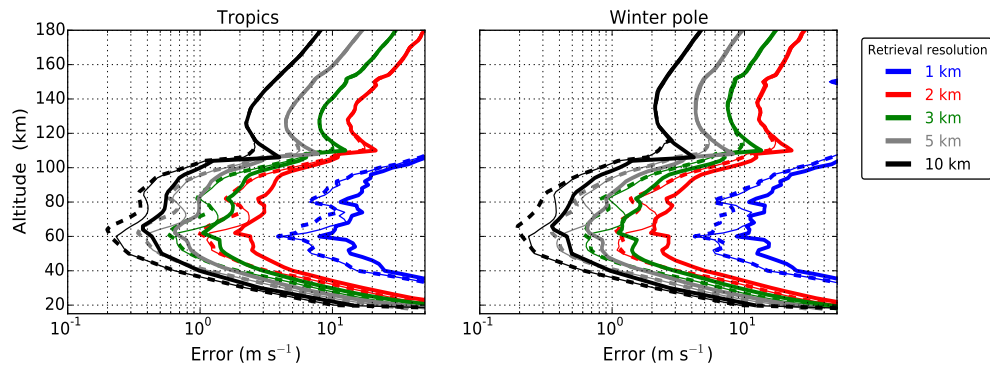

Figure 15. Error profiles for retrievals with different vertical resolutions. The full lines show the errors for composite profiles derived from bands at 487/552 GHz, 625/655 GHz and 2 THz. The dashed lines show the composite profiles for the alternative bands: 487/552 GHz, 627/654 GHz (8 GHz bandwidth) and 2 THz. Calculations are performed for night-time tropical atmosphere with the observation parameters in Tab 2. The thin lines are the alternative-bands error profiles for day time.

it is the best spectral range for measuring winds between 40 and 70 km.[15] A spectrometer with bandwidth of 8 GHz could allow to measure bands 3 and 4 together with the 655 GHz lines.

We also investigate the retrieval performances using the H2O and CO lines at 557 GHz and 577 GHz, respectively. The lines can be measured in the same DSB spectrum with a relatively narrow spectral bandwidth and a high spectral resolution of 0.25 MHz. Here we use a 2 GHz bandwidth in order to include other lines such as a strong O_3, a N_2O and HO_2 lines (Fig. 7). The water vapour line is the strongest line in the sub-millimeter spectrum (frequencies below 1-THz) and it is then the most suitable line for measuring upper-mesospheric and lower-thermospheric winds. The band provides high sensitive water vapour and CO measurements from the middle stratosphere to the lower thermosphere.[16, 17, 24–26] Temperature can also be retrieved from 20 to 90 km.[26, 27]

Estimates of the wind retrieval errors from the alternative bands herebelow, are shown in Fig. 14.

- 624/652 GHz, DSB with 8 GHz bandwidth and 1 MHz resolution

- 557/577 GHz, DSB with 2 GHz bandwidth and 0.25 MHz resolution

Significant improvements are found between 35 to 100 km compared to the default bands definition. The 655 GHz O_3 lines allow to retrieve the line-of-sight winds between 45 and 70 km with an error of 2 m s^{-1} and a vertical resolution of 2 km. Above 60 km, the retrieval performances are degraded in daytime because of the O_3 mesospheric diurnal variation. From the 557 GHz H_2O line, profiles are retrieved in the tropics between 60 to 95 km with an error better than 5 m s^{-1} and a vertical resolution of 2 m s^{-1}. The altitude range of the good retrievals clearly depends on the H_2O spatial distribution driven by the summer-pole to winter-pole upper atmospheric circulation. Similarly, the measurement sensitivity in the lower thermosphere increases in the winter pole due to the descent of the thermopheric CO.

The results obtained from the different settings are summarized in Fig. 14. The composite error profiles are derived from the default and the alternative bands, respectively. The alternative bands include the original 487/527 GHz bands. The O_2 lines at 487 GHz is important to measure temperature and tangent-height pressure below about 90 km.[28] The 527 GHz band is the most suited band among the selected ones for observing the upper-troposphere and lower stratosphere. However if only 4 SMM bands have to be selected, the two alternative bands alone could be considered. With such setting, the radiometer is compatible with the current mission design and will allow to fulfil most of the scientific objectives. Indeed, first estimations show that temperature and tangent-height pressure can be retrieved with good performances from the alternative bands without the O_2 line, and most of the molecules observed at 527 GHz can also be measured in other bands (but with less sensitivity in the upper troposphere).

5. CONCLUSION

The sub-millimeter limb sensor JEM/SMILES with a radiometer cooled at 4 K, demonstrated the capacity of such technologies to measure middle-atmospheric horizontal winds with good precision. A good agreement is found between SMILES zonal winds and ECMWF operational analyses in the stratosphere at mid-latitudes (differences <2 m s^{-1} on daily and zonally averaged winds). On the other hand, clear differences (>5 m s^{-1}) are seen in regions where ECMWF analyses are expected to have difficulties to reproduce the winds, i.e. in the Tropics and globally, in the mesosphere. The main error sources on SMILES retrievals have been discussed to help at the preparation of future missions.

SMILES-2 is under study in Japan. The first quantitative assessment of its capability for measuring winds has been presented. It is shown that line-of-sight winds can be retrieved from 20 km to more than 180 km. In its current definition, the best sensitivity is found between 40–90 km where winds can be retrieved with a precision better than 5 m s^{-1} and a vertical resolution of 2 km. It is a region where the current wind observation techniques lack sensitivity and, SMILES-2 can also be considered as a good complement of the future spaceborne wind lidar missions devoted to the troposphere and lower stratosphere such as ADM. Between 110 and 160 km,

winds can be measured with a precision better than 10 m s^{-1} and a vertical resolution better than 5 m s^{-1}. These performances are slightly inferior than those of the future mission ICON/MIGHTI, but unlike the latter, SMILES-2 can perform day and night wind measurements.

An alternative definition of the spectral bands have been discussed to improve the wind retrievals between 35–100 km. It is proposed to increase the bandwidth of bands 3–4 (625/650 GHz) in order to measure a dense cluster of strong O_3 lines at 655 GHz and to add a new pair of bands at 557 and 577 GHz for upper atmospheric H2O and CO measurements, respectively. Using the alternative bands, wind retrieval precision can be increased by a factor 2.

At 30 km, the precision is only 10 m s^{-1}. It can be improved only by using very large spectral bandwidth (>16 GHz) in order to increase the number of molecular lines with moderate intensities. Such setting is not considered for SMILES-2.

The simulation study is still in progress. The errors analysis is being improved in order to provide requirements on the acceptable uncertainty levels on intensity calibration, sideband spectral filter and line-of-sight velocity correction. These studies need to take into account the retrievals of other parameters (temperature, molecular abundances, line-of-sight tangent height). New retrieval algorithms are developed in order to handle the large number of measurements data and the retrieval parameters compared to JEM/SMILES. It is also important to take into account the different physical properties of the middle atmosphere (altitudes below 100 K) and the thermosphere. On going analyses also include the improvements of the radiative transfer model used for JEM/SMILES analysis in order to study potential effects of non-local thermodynamic equilibrium in the thermosphere and the line Zeeman splitting of the molecular and atomic oxygen lines.[29,30] An assimilation experiment is also discussed to quantitatively assess the impacts of SMILES-2 on atmospheric models such as chemical transport or weather prediction models. The results will provide better insights of the observation requirements such as the vertical resolution and precision of the measurements, the horizontal sampling, orbit inclination. The use of two perpendicular line-of-sights to infer the 2-D horizontal wind vector, is also discussed. A minimalist definition of SMILES-2 with a reduced number of spectral bands and a radiometer cooled at 70 K is also discussed.

Acknowledgments

REFERENCES

[1] Baldwin, M., Thompson, D., Shuckburgh, E., Norton, W., and Gillett, N., "Weather from the stratosphere?," *Science* **301**, 317–318 (2003).

[2] Shepherd, G. G., "Development of wind measurement systems for future space missions," *Acta Astronautica* **115**, 206 – 217 (2015).

[3] Jin, H., Miyoshi, Y., Fujiwara, H., Shinagawa, H., Terada, K., Terada, N., Ishii, M., Otsuka, Y., and Saito, A., "Vertical connection from the tropospheric activities to the ionospheric longitudinal structure simulated by a new earth's whole atmosphere-ionosphere coupled model," *Journal of Geophysical Research: Space Physics* **116**(A1) (2011).

[4] Lahoz, W. A., Brugge, R., Jackson, D. R., Migliorini, S., Swinbank, R., Lary, D., and Lee, A., "An observing system simulation experiment to evaluate the scientific merit of wind and ozone measurements from the future SWIFT instrument," *Quarterly Journal Of The Royal Meteorological Society* **131**(606), 503–523 (2005).

[5] Stoffelen, A., Pailleux, J., Källén, E., Vaughan, J., Isaksen, L., Flamant, P., Wergen, W., Andersson, E., Schyberg, H., Culoma, A., Meynart, R., Endemann, M., and Ingmann, P., "The atmospheric dynamics mission for global wind field measurement," *Bull. Amer. Meteor. Soc.* **86**, 73–87 (2005).

[6] Barath, F. T., Chavez, M. C., Cofield, R. E., Flower, D. A., Frerking, M. A., Gram, M. B., Harris, W. M., Holden, J. R., Jarnot, R. F., Kloezeman, W. G., Klose, G. J., Lau, G. K., Loo, M. S., Maddison, B. J., Mattauch, R. J., McKinney, R. P., Peckham, G. E., Pickett, H. M., Siebes, G., Soltis, F. S., Suttie, R. A., Tarsala, J. A., Waters, J. W., and Wilson, W. J., "The upper atmosphere research satellite microwave limb sounder instrument," *Journal of Geophysical Research: Atmospheres* **98**(D6), 10751–10762 (1993).

[7] Murtagh, D., Frisk, U., Merino, F., Ridal, M., Jonsson, A., Stegman, J., Witt, G., Eriksson, P., Jimenez, C., Mégie, G., de la Noë, J., Ricaud, P., Baron, P., Pardo, J., Hauchcorne, A., Llewellyn, E., Degenstein, D., Gattinger, R., Lloyd, N., Evans, W., McDade, I., Haley, C., Sioris, C., von Savigny, C., Solheim, B., McConnell, J., Strong, K., Richardson, E., Leppelmeier, G., Kyrola, E., Auvinen, H., and Oikarinen, L., "An overview of the Odin atmospheric mission," *Can. J. Phys.* **80**, 309–319 (APR 2002).

[8] Kikuchi, K., Nishibori, T., Ochiai, S., Ozeki, H., Irimajiri, Y., Kasai, Y., Koike, M., Manabe, T., Mizukoshi, K., Murayama, Y., Nagahama, T., Sano, T., Sato, R., Seta, M., Takahashi, C., Takayanagi, M., Masuko, H., Inatani, J., Suzuki, M., and Shiotani, M., "Overview and early results of the Superconducting Submillimeter-Wave Limb-Emission Sounder (SMILES)," *J. Geophys. Res.* **115**(D23), D23306 (2010).

[9] Wu, D. L., Schwartz, M. J., Waters, J. W., Limpasuvan, V., Wu, Q. A., and Killeen, T. L., "Mesospheric doppler wind measurements from Aura Microwave Limb Sounder (MLS)," *Advances In Space Research* **42**(7), 1246–1252 (2008).

[10] Baron, P., Murtagh, D. P., Urban, J., Sagawa, H., Ochiai, S., Kasai, Y., Kikuchi, K., Khosrawi, F., Körnich, H., Mizobuchi, S., Sagi, K., and Yasui, M., "Observation of horizontal winds in the middle-atmosphere between 30S and 55N during the northern winter 2009–2010," *Atmospheric Chemistry and Physics* **13**(13), 6049–6064 (2013).

[11] Rüfenacht, R., Kämpfer, N., and Murk, A., "First middle-atmospheric zonal wind profile measurements with a new ground-based microwave doppler-spectro-radiometer," *Atmos. Meas. Techn.* **5**(11), 2647–2659 (2012).

[12] Manago, N., Ozeki, H., and Suzuki, M., "Band selection study for the sub-MM limb sounder, SMILES-2.," *IEEE Geoscience and Remote Sensing Symposium, 13-18 July, Quebec City*, 4153–4156 (2014).

[13] Manago, N., Baron, P., Ochiai, S., Ozeki, H., and Suzuki, M., "Sensitivity study of SMILES-2 for chemical species," *Proc. of SPIE Remote sensing* **9639-22** (2015).

[14] Ochiai, S., Uzawa, Y., Irimajiri, Y., Baron, P., Nishibori, T., Manabe, T., Mizuno, A., Nagahama, T., Fujii, Y., Suzuki, M., and Shiotani, M., "Planned submillimeter limb sounder (SMILES-2) for measurement of temperature, wind, and chemical species in the middle atmosphere," *Proc. of SPIE Remote sensing* **9639-21** (2015).

[15] Baron, P., Murtagh, D. P., Urban, J., Sagawa, H., Eriksson, P., and Ochiai, S., "Definition of an uncooled submillimeter/thz limb sounder for measuring middle atmospheric winds.," *ESA Living Planet Symposium, 9-13 September, Edinburgh (UK)*, 1–8 (2013).

[16] Merino, F., Murtagh, D., Ridal, M., Eriksson, P., Baron, P., Ricaud, P., and de la Noë, J., "Studies for the Odin Sub-Millimetre Radiomoter: III. Performance simulations," *Can. J. Phys.* **80**, 357–373 (APR 2002).

[17] Urban, J., Lautié, N., Murtagh, D., Eriksson, P., Kasai, Y., Lossow, S., Dupuy, E., de La Noë, J., Frisk, U., Olberg, M., Flochmoën, E. L., and Ricaud, P., "Global observations of middle atmospheric water vapour by the odin satellite: An overview," *Planetary and Space Science* **55**(9), 1093 – 1102 (2007). Highlights in Planetary Science 2nd General Assembly of Asia Oceania Geophysical Society.

[18] Roelfsema, P. R., Helmich, F. P., Teyssier, D., Ossenkopf, V., Morris, P., Olberg, M., Shipman, R., Risacher, C., Akyilmaz, M., Assendorp, R., Avruch, I. M., Beintema, D., Biver, N., Boogert, A., Borys, C., Braine, J., Caris, M., Caux, E., Cernicharo, J., Coeur-Joly, O., Comito, C., de Lange, G., Delforge, B., Dieleman, P., Dubbeldam, L., de Graauw, Th., Edwards, K., Fich, M., Flederus, F., Gal, C., di Giorgio, A., Herpin, F., Higgins, D. R., Hoac, A., Huisman, R., Jarchow, C., Jellema, W., de Jonge, A., Kester, D., Klein, T., Kooi, J., Kramer, C., Laauwen, W., Larsson, B., Leinz, C., Lord, S., Lorenzani, A., Luinge, W., Marston, A., Martn-Pintado, J., McCoey, C., Melchior, M., Michalska, M., Moreno, R., Mller, H., Nowosielski, W., Okada, Y., Orleaski, P., Phillips, T. G., Pearson, J., Rabois, D., Ravera, L., Rector, J., Rengel, M., Sagawa, H., Salomons, W., Snchez-Surez, E., Schieder, R., Schlder, F., Schmlling, F., Soldati, M., Stutzki, J., Thomas, B., Tielens, A. G. G. M., Vastel, C., Wildeman, K., Xie, Q., Xilouris, M., Wafelbakker, C., Whyborn, N., Zaal, P., Bell, T., Bjerkeli, P., de Beck, E., Cavali, T., Crockett, N. R., Hily-Blant, P., Kama,

M., Kaminski, T., Leflch, B., Lombaert, R., De Luca, M., Makai, Z., Marseille, M., Nagy, Z., Pacheco, S., van der Wiel, M. H. D., Wang, S., and Yldz, U., "In-orbit performance of Herschel-HIFI," *A&A* **537**, A17 (2012).

[19] Rodgers, C. D., [*Inverse Methods for Atmospheric Sounding: Theory and Practise*], vol. 2 of *Series on Atmospheric, Oceanic and Planetary Physics*, World Scientific (2000).

[20] Urban, J., Baron, P., Lautié, N., Schneider, N., Dassas, K., Ricaud, P., and De La Noë, J., "MOLIERE (v5): a versatile forward- and inversion model for the millimeter and sub-millimeter wavelength range," *J. Quant. Spectrosc. Ra.* **83**, 529–554 (FEB 1 2004).

[21] Baron, P., Mendrok, J., Kasai, Y., Ochiai, S., Seta, T., Sagi, K., Suzuki, K., Sagawa, H., and Urban, J., "AMATERASU: Advanced Model for Atmospheric TErahertz Radiation Analysis and Simulation," *Journal of the National Institute of Information and Communications Technology* **55 (1)**, 109–121 (2008).

[22] Baron, P., Urban, J., Sagawa, H., Möller, J., Murtagh, D. P., Mendrok, J., Dupuy, E., Sato, T. O., Ochiai, S., Suzuki, K., Manabe, T., Nishibori, T., Kikuchi, K., Sato, R., Takayanagi, M., Murayama, Y., Shiotani, M., and Kasai, Y., "The level 2 research product algorithms for the Superconducting Submillimeter-Wave Limb-Emission Sounder (SMILES)," *Atmos. Meas. Techn.* **4**(10), 2105–2124 (2011).

[23] Rothman, L., Gordon, I., Barbe, A., Benner, D., Bernath, P., Birk, M., Boudon, V., Brown, L., Campargue, A., Champion, J.-P., Chance, K., Coudert, L., Dana, V., Devi, V., Fally, S., Flaud, J.-M., Gamache, R., Goldman, A., Jacquemart, D., Kleiner, I., Lacome, N., Lafferty, W., Mandin, J.-Y., Massie, S., Mikhailenko, S., Miller, C., Moazzen-Ahmadi, N., Naumenko, O., Nikitin, A., Orphal, J., Perevalov, V., Perrin, A., Predoi-Cross, A., Rinsland, C., Rotger, M., imekov, M., Smith, M., Sung, K., Tashkun, S., Tennyson, J., Toth, R., Vandaele, A., and Auwera, J. V., "The HITRAN 2008 molecular spectroscopic database," *Journal of Quantitative Spectroscopy and Radiative Transfer* **110**(910), 533 – 572 (2009). HITRAN.

[24] Dupuy, E., Urban, J., Ricaud, P., Le Flochmoën, E., Lautié, N., Murtagh, D., De La Noë, J., El Amraoui, L., Eriksson, P., Forkman, P., Frisk, U., Jégou, F., Jiménez, C., and Olberg, M., "Strato-mesospheric measurements of carbon monoxide with the Odin Sub-Millimetre Radiometer: Retrieval and first results," *Geophysical Research Letters* **31**(20) (2004).

[25] Lossow, S., Urban, J., Gumbel, J., Eriksson, P., and Murtagh, D., "Observations of the mesospheric semi-annual oscillation (MSAO) in water vapour by Odin/SMR," *Atmos. Chem. Phys.* **8**(21), 6527–6540 (2008).

[26] Christensen, O. M., Eriksson, P., Urban, J., Murtagh, D., Hultgren, K., and Gumbel, J., "Tomographic retrieval of water vapour and temperature around polar mesospheric clouds using Odin-SMR," *Atmospheric Measurement Techniques* **8**(5), 1981–1999 (2015).

[27] Baron, P., Merino, F., and Murtagh, D., "Simultaneous retrievals of temperature and volume mixing ratio constituents from nonoxygen Odin submillimeter radiometer bands," *Appl. Opt.* **40**, 6102–6110 (Nov 2001).

[28] Manago, N., Baron, P., Ochiai, S., Ozeki, H., and Suzuki, M., "Upper-stratosphere/mesosphere temperature, wind speed, H2O and O3 measurements using sub-MM limb sounder," *IEEE Geoscience and Remote Sensing Symposium, 26–31 July, Milan (It)* (2015).

[29] Abragam, A. and Van Vleck, J. H., "Theory of the microwave zeeman effect in atomic oxygen," *Phys. Rev.* **92**, 1448–1455 (Dec 1953).

[30] Pardo, J. R., Ridal, M., Murtagh, D., and Cernicharo, J., "Microwave temperature and pressure measurements with the odin satellite: I. observational method," *Canadian Journal of Physics* **80**(4), 443–454 (2002).